PERGAMON

Journal of Structural Geology 24 (2002) 339–357

JOURNAL OF STRUCTURAL GEOLOGY

www.elsevier.com/locate/jstrugeo

Evolution of an eclogitized continental fragment in the Eastern Alps (Sieggraben, Austria)

Marián Putiš[a,1,*], Sergei P. Korikovsky[b], Eckart Wallbrecher[c], Wolfgang Unzog[c], Niels Ø. Olesen[d], Harald Fritz[c]

[a]*J.A. Comenius University of Bratislava, Faculty of Natural Sciences, Dept. of Mineralogy and Petrology, Mlynska dolina, SK-84215 Bratislava, Slovak Republic*

[b]*Russian Academy of Sciences, Institute of Geology of Ore Deposits, Petrography, Mineralogy and Geochemistry, Staromonetny per. 35, 109017 Moscow, Russian Federation*

[c]*K.F. University of Graz, Institute of Geology and Paleontology, Heinrichstr. 26, A-8010 Graz, Austria*

[d]*University of Århus, Faculty of Science, Dept. of Earth Sciences, Nordre Ringgade 1, DK-8000 Århus, Denmark*

Received 3 November 1999; revised 26 March 2001; accepted 31 May 2001

Abstract

The sequence of tectonometamorphic events that developed in continental basement rocks during the Alpine orogeny was studied in the eclogitic Sieggraben structural complex (SSC) in the Austrian Eastern Alps. The eclogitization of a pre-Alpine basement fragment occurred during Early Cretaceous when this was collisionally buried at the depth of ca. 50–55 km with an estimated mean temperature of 720°C at about 15 kbar (D1). Thermal relaxation under increasing temperatures to ca. 770°C and slightly decreasing pressures resulted in rapid exhumation recorded by symplectitic intergrowth of $Cpx2_{Jd3\text{-}22}$ and Pl2 in eclogites and HP amphibolites. The exhumation was enhanced by the dynamic strain softening of prograde metamorphic Om_{Jd38} and Zo1 into an aggregate of minor $Cpx2_{Jd18\text{-}31}$ and Zo2. Dynamic recrystallization of Hbl1, feldspars and Qtz ribbons at high- to medium-temperatures was followed by medium- to low-temperature Qtz recrystallization and Cal twinning. The textures indicate dislocation creep as the principal micromechanism of ductile deformation of Cpx, Am, Pl and Qtz, or dominated mechanical twinning in Cal. Textural patterns are mainly related to high–medium temperature mesoscopic fabrics (D2). Compressional exhumation along a detachment fault initiated top-to-SSE extensional unroofing of the eclogitized SSC now overlying the low-grade MP/HP Lower Austro–Alpine structural complexes.

Keywords: Eclogites; Fragment; Dislocation creep; Eastern Alps

1. Introduction

This paper describes Alpine reactivation of basement rocks within a major Cretaceous shear zone reconstructed in the Austro–Alpine (AA) unit internides in the Austrian territory (Fig. 1), comprising different structural complexes, among which the Middle AA were reactivated under eclogite facies conditions. We try to determine how observed small-scale structures translate into large scale features in reactivation tectonics.

The principal tectonic zones and lines within the East Alpine–Carpathian collisional orogen are shown in Fig. 1. Area 1 belongs to the Tertiary ALCAPA (Alps–Carpathians–Pannonia) Megablock comprising the Eastern Alps, Western Carpathians and Pannonian Basin. The ALCAPA Megablock contains a large volume of the pre-Mesozoic basement complexes incorporated into Mesozoic and Tertiary tectonic structures. Some of the basement fragments bear features of collisional suture zones, indicating structural–metamorphic reactivation under amphibolite to eclogite-facies conditions.

The analysis of an early Cretaceous major shear zone in the internal part of the Eastern Alps was performed by a study of meso- and microfabrics in the southeastern AA structural complexes. Most of the attention has been paid to the Middle AA Sieggraben structural complex (Kümel, 1935; Tollmann, 1977; Putiš, 1992) reactivated under eclogite-facies conditions.

This paper deals with the 'thick-skinned' tectonics within the AA domain and with microstructural–textural evolution in natural tectonites during reactivation.

* Corresponding author. Fax: +4217-60296293.
E-mail address: putis@fns.uniba.sk (M. Putiš).

[1] Temporary address: Denmark Technical University, Institute of Geology and Geotechnical Engineering, DK-2800 Copenhagen-Lyngby, Denmark.

0191-8141/01/$ - see front matter
PII: S0191-8141(01)00071-2

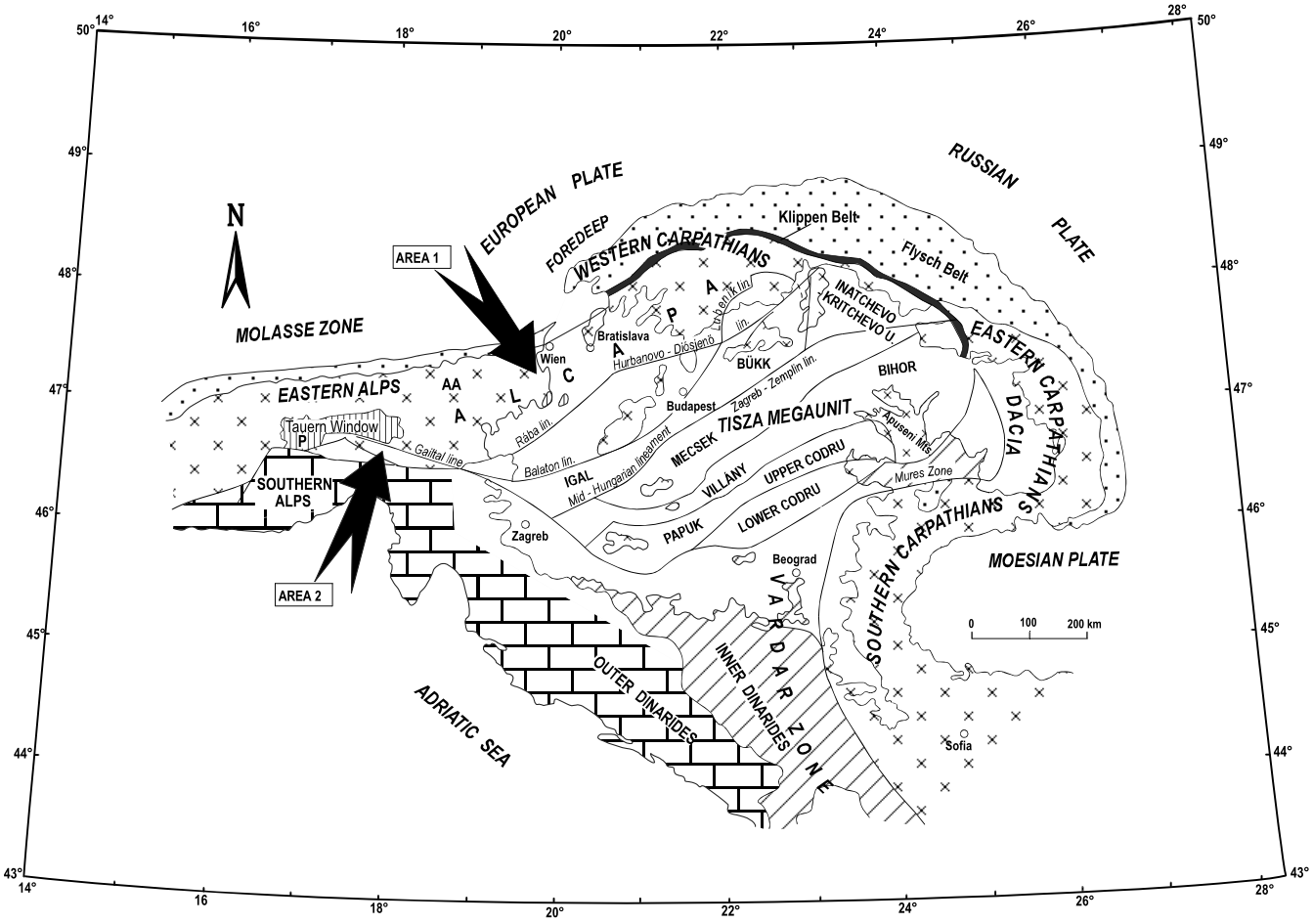

Fig. 1. Tectonic sketch map of the East Alpine–Carpathian (ALCAPA) orogen with position of the Austro–Alpine (AA) unit (Plašienka et al., 1997). Area 1: Sieggraben structural complex. Area 2: Kreuzeck Massif AA structural complex SE of Tauern Window (data under completion).

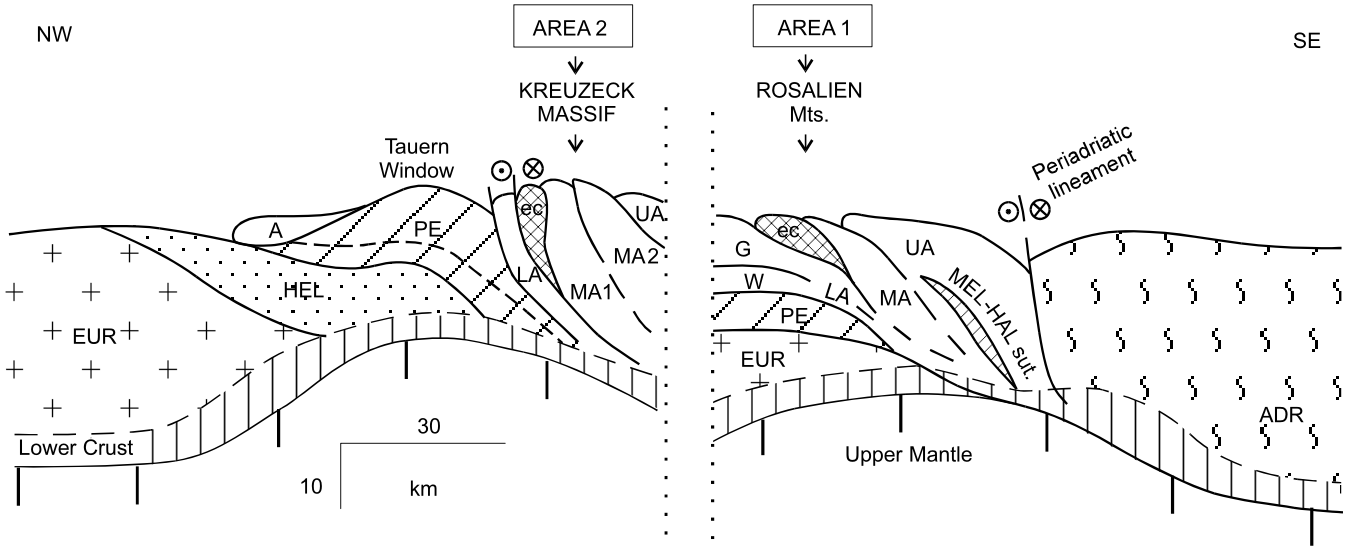

Fig. 2. Schematic tectonic cross-section of the investigated Area 1 (and Area 2 under completion). EUR = European plate, HEL = Helvetic structural complex (SC), PE = Pennine SC, A = Austro–Alpine unit with the LA = Lower AA Grobgneis (G) and Wechsel (W) SC, MA = Middle AA SC, UA = Upper AA SC, MEL–HAL sut. = Meliata–Hallstatt Ocean suture zone, ADR = Adria (or Apulia) microplate, ec = eclogite-bearing complex.

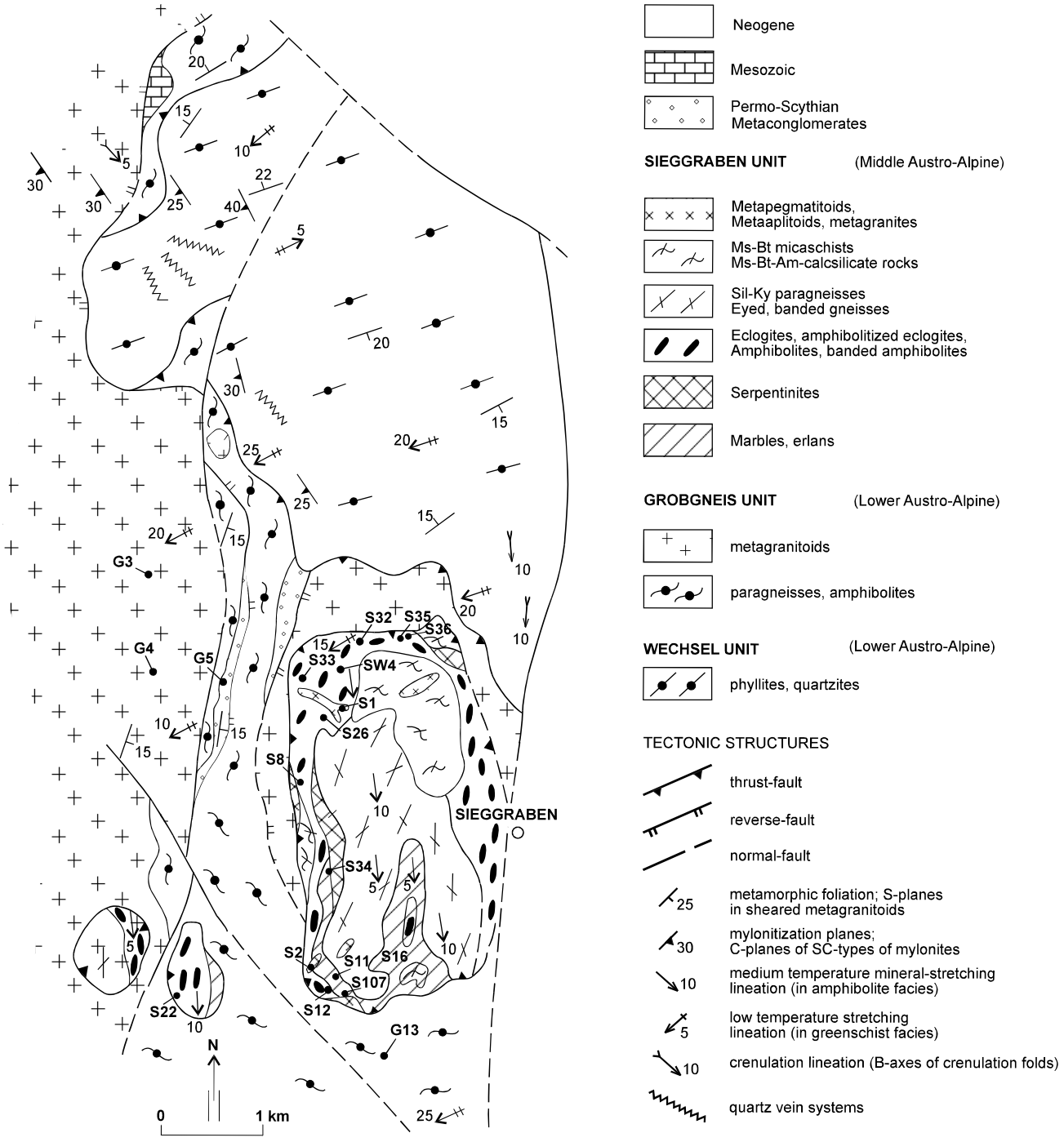

Fig. 3. Geological-tectonic sketch-map of the Middle and Lower Austro–Alpine basement and cover complexes in the Sieggraben area (Putiš, 1992).

2. Methods

This paper follows detailed field mapping (the Austrian Geological Survey mapping program 1991–1994, attended by M. Putiš) and recently performed complementary structural, petrological and geochronological studies. Minerals were analyzed in polished sections using CAMSCAN electron microprobe equipped with a LINK H.E.D.A. system. For obtaining *PT*-estimates, we used equilibrium mineral assemblages of the D1 and D2 stages (most used microprobe analyses after Putiš et al. (2000)) in different thermobarometers. The textural (CPO) patterns of omphacite, zoisite, amphibole, plagioclase, quartz and calcite were measured by U-stage. A reflection X-ray texture goniometer was used for Qtz and Cal. SEM (CamScan) in EBS mode was used for the study of grain boundaries and fine-grained

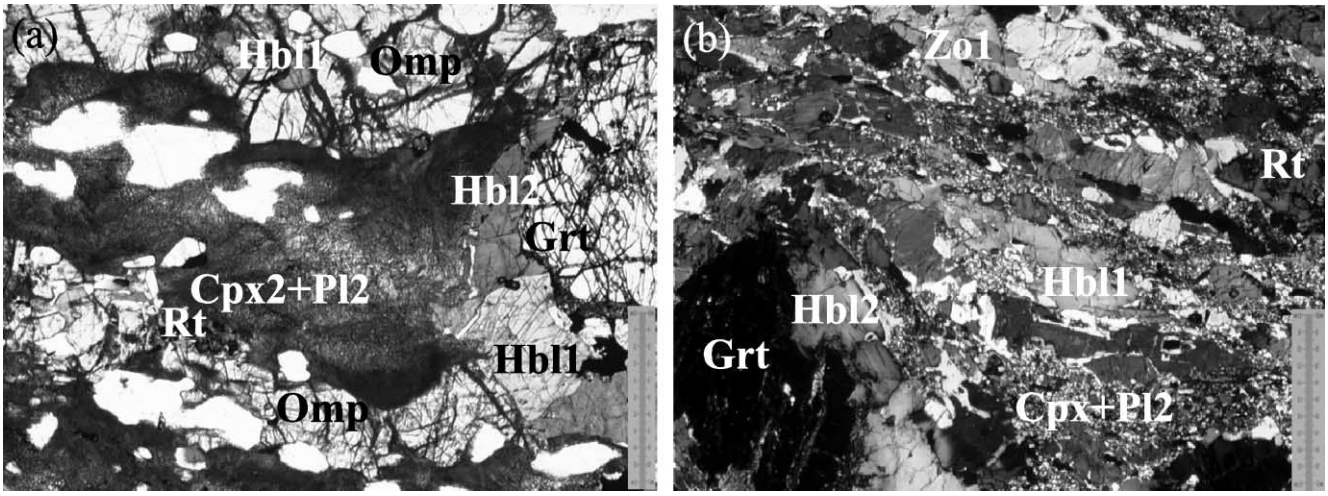

Fig. 4. Reaction recrystallization microstructures of eclogite and HP amphibolite (the Sieggraben SC). (a) Prismatic Cpx1–Omp associated with Rt, ±Hbl1 and Grt (D1); fine-grained reactional (D2) symplectite of Cpx2 and Pl, eclogite (s. S35). (b) Prismatic Hbl1 associated with Rt, Zo and Grt (D1); fine-grained reactional (D2) symplectite of Cpx and Pl, and Hbl2, HP amphibolite (s. S26). 1 mm scale displayed.

mineral aggregates. Mineral abbreviations (see Appendix A) in text and figures are used after Kretz (1983) and end-members of Ca-amphiboles after Leake et al. (1997).

3. Geological setting of the Sieggraben structural complex

The Sieggraben structural complex (SSC) was studied near the villages of Sieggraben and Schwarzenbach, about 80 km south of Vienna (Fig. 1). Tectonostratigraphy of the Middle Austro–Alpine (MAA) and Lower Austro–Alpine (LAA) structural complexes (Tollmann, 1977) as well as the field relationships of superimposed macrostructures in the area considered (Putiš, 1992) are outlined in Figs. 2 and 3. The top of the tectonostratigraphic profile is occupied by the MAA SSC, overlying the LAA Grobgneis and Wechsel structural complexes as the result of Early Cretaceous collision. The MAA Sieggraben eclogites belong to a gneiss–amphibolite–serpentinite–marble lithological complex with some concordant to discordant veins of granitic–pegmatitic orthogneiss. Eclogitic lenses are commonly located within the ductile banded amphibolites or marbles.

Low-angle normal faults in the footwall of the Sieggraben and Grobgneis structural complexes are younger, probably Late Cretaceous–Early Tertiary structures. Accompanying low-temperature *S–C* mylonites indicate top-to-WSW movement along low-temperature stretching lineations defined by newly formed white mica, Bt and Chl.

An older, Early Cretaceous higher-temperature extensional fabric is formed by parallel NNW–SSE directed D1 mineral and D2 stretching lineations and ductile layered structures. These are only recognizable in the internal part of the MAA SSC.

Taking into account the zircon–monazite U–Pb-upper discordia intercept- and whole-rock Rb–Sr isotope ages of the Sieggraben orthogneisses, 312 ± 8 Ma or 289 ± 16 Ma, respectively (Putiš et al., 2000), an Early Paleozoic age is inferred for the MAA Sieggraben lithological complex as a minimum age. No relics of the pre-Alpine metamorphism have been preserved. The Alpine reactivation of the SSC is also well constrained by the U–Pb isotope study of zircon and monazite of granitic orthogneisses of the complex. The U–Pb lower discordia intercept age of about 103 Ma (Putiš et al., 1998, 2000) using zircon and monazite from the Sieggraben orthogneiss is interpreted to either date the cooling of the SSC during the thrusting along a deep crustal detachment fault, between 750 and 500°C, or to indicate the achieved maximum reactivation temperatures at around 770°C. A similar intercept age of the underlying LAA Wechsel structural complex Wiesmath orthogneiss is interpreted to date contemporaneous Alpine metamorphism of the buried LAA structural complexes with the maximum temperatures slightly over 500°C at 10 kbar, calculated by Grt–Chl and Grt–Bt thermometers and Phe barometer (Korikovsky et al., 1998). This time period overlaps with the shortening period within the Meliata–Hallstatt basin passive continental margin that is also well defined in the Western Carpathians Veporic mid-Cretaceous structural complex (Putiš, 1991; Dallmeyer et al., 1996).

4. Metamorphic and deformational microfabrics of mylonitized rocks

4.1. Eclogites and HP amphibolites

4.1.1. Low strain domains

Metabasites in the area are locally developed as eclogites composed of pale-green or colourless Omp, Grt, Zo and Rt;

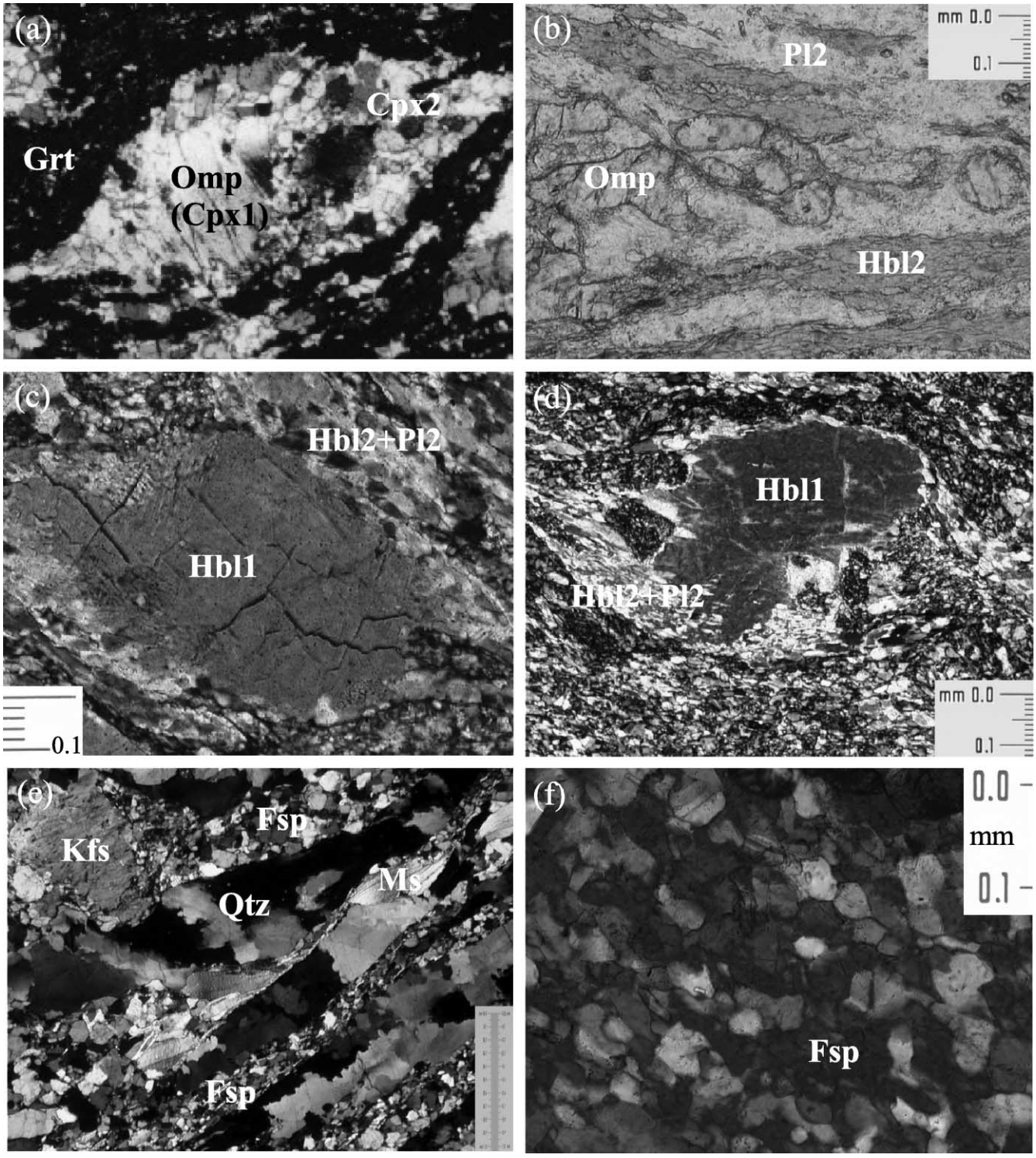

Fig. 5. Higher-*T* microstructures of mylonites (the Sieggraben SC). (a) Omp (Cpx1) surrounded by mantle of Cpx2 (early D2), (s. Zob1), 7 mm = 300 μm. (b) Brittle shear in Omp porphyroclast surrounded by Hbl2 and Pl2 aggregate (D2), layered HP amphibolite (s. S22). (c and d) Sigmoidal (top-to-SSE) Hbl1 porphyroclasts within the Hbl2 and Pl2 (D2) aggregate, HP amphibolite–mylonite (s. S22). (e) Migration recrystallization of Qtz ribbons; rotation recrystallization of feldspar bands (D2), granitic orthogneiss–mylonite (s. S1). (f) Partly equilibrated new grains of Pl(2) and Kfs(2) within recrystallized feldspar aggregate (s. S1).

most of them are eclogitized HP amphibolites with the transitional textures to eclogites. They contain 0.5–1 cm large prismatic blasts of $Cpx1_{Jd26\text{-}38}$ (Omp) grown within the medium-grained amphibolitic matrix composed of brown-green Hbl(1), Grt, Rt, Zo1, with a small amount of Pl1 and rare Ep. Omp porphyroblasts contain irregularly shaped inclusions of Hbl1 (Prg, Hs), Rt, Zo1, even less Pl1 or Ep, and sometimes have a diablastic texture (Fig.

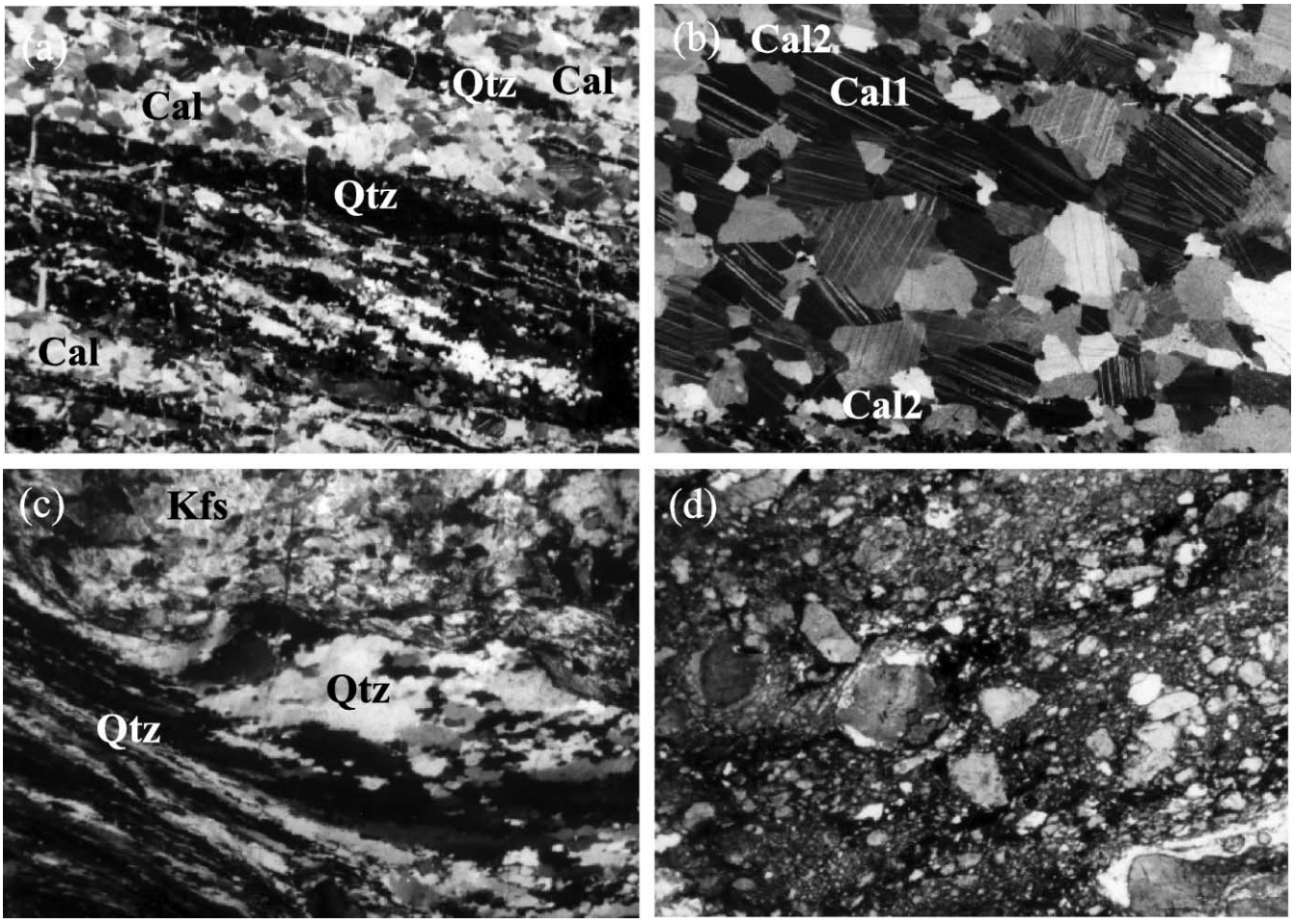

Fig. 6. Lower-*T* microtextures of mylonites (the Sieggraben SC). (a) Qtz ribbons recrystallized along the boundaries (late D2), quartz lense in marble (s. S107). (b) Flattening of Cal grains parallel to e-lamellae (late D2); S foliation//e is cut by *C*-planes marked by (minor) Cal(2) grains, marble (s. S11). (c) Recrystallized ribbons to narrow band and fibres of Qtz (late D3) indicating top-to-WSW extensional shearing, *S*–*C* mylonite of the Grobgneis granite (s. G13). (d) Cataclastic structure of eclogite (s. S36). Magnification: 27× (b–d), 7.5× (a).

4a). Omp thus progressively overgrew Hbl1, Rt, Zo1, Ep, Pl1 and Grt, a mineral assemblage representing the HP amphibolite. This overgrowth represents the D1 progressive burial stage of the SSC. Omp and Hbl1 define a (D1) metamorphic lineation in eclogites and HP amphibolites.

High-pressure Omp and Hbl1 are rimmed or partly replaced by very fine-grained symplectitic aggregates of Cpx2 ($Jd_{3\text{-}22}$, 5–40 μm in size) and Pl2 (10–30 μm, locally 100 μm); Rt is rimmed by Ilm and/or Ttn (Fig. 4b). They are interpreted to reflect the high-temperature part of the D2 exhumation stage. Macroscopically, the Cpx2 and Pl2 aggregates are separated into pale-green lenses and layers around Cpx1 (Omp) or Hbl1 (Prg and Hs) prismatic porphyroclasts, parallel to NNW–SSE trending (D1) mineral and (D2) stretching lineations.

4.1.2. High strain domains

Some eclogites display a layered structure with red-pinkish layers of Grt, pale-green layers of Omp dynamically recrystallized into aggregate of higher-$Jd_{18\text{-}31}$ Cpx2 and white layers of Zo, a little Pl and Qtz, as well as rare dark layers of Am. The Cpx2-bearing layers consist of isometric minor (ca. 100 μm) grains with frequent sigmoidally rotated Omp relict cores, mantled by equidimensional mostly omphacitic Cpx2 (Fig. 5a), coexisting with synkinematically grown Grt. The microstructure is interpreted to represent the initial stage of extensional exhumation (D2 stage) and is inferred for the hanging wall of the SSC thrust.

The HP amphibolites are transformed into layered amphibolites and mylonites. The dark layers are composed of relic cores or porphyroclasts (mainly 300–600 μm) of dynamically recrystallized Hbl1 surrounded by a fine-grained (20–40 μm) Hbl2 (Prg + Hb or Prg + Act) mantle (Fig. 5b–d). White layers were formed by dynamic recrystallization of Pl1 into aggregates composed of Pl2 (5–40 μm) with a lesser amount of Qtz.

Amphibolites and layered mylonitic amphibolites contain a smaller amount of Cpx1–Omp, which behaved as a mechanically resistant phase within the newly formed surrounding mylonitic matrix composed of Hbl2 (Prg +

Hb or Act) and Pl2 as a product of dynamic recrystallization of Hbl1 and Pl1. Cpx clasts are segmented by many tension fractures and microshears (Fig. 5b). This indicates high- but mainly medium-*T* deformation conditions during the D2 exhumation stage, when Am and Pl (with Qtz) were strain accommodating phases. Laminated ultramylonites contain about 90% of dynamically recrystallized matrix enclosing Hbl1 (Hb or Ed) and rare mantled Omp porphyroclasts. Dynamic recrystallization of Hbl(1) started as an evolution of the mantled structures. Sigmoidally rotated Hbl1 porphyroclasts show tails of dynamically recrystallized Hbl2 (Prg + Hb or Prg + Act) aggregates mixed with Pl2 (Fig. 5c and d). The asymmetrical microstructures are consistent with top-to-SSE extensional sliding (D2), also evident from mesoscopic structures.

Superimposed (late D2) *S–C* microfabrics (Berthé et al., 1979) associated with the greenschist-facies recrystallization (Chl, Bt, Cal, Ep–Czo, Ab, Qtz) are rare. Most of low-*T* minerals belong to D3 deformation or top-to-the-WSW extensional sliding, coeval with the same structures in the footwall Grobgneis and Wechsel LAA structural complexes. Ultracataclasite (Putiš et al., 2000) develops in eclogites at the base of the SSC (Fig. 6d) during the latest stages of deformation.

4.2. Granitic–pegmatitic orthogneisses

The coarse-grained texture of primary (Variscan) Grt–Ms–Kfs–Pl–Qtz–Tur mineral association of pegmatoid shows transitions into a medium-temperature Alpine *S–C* mylonite. Newly-formed micas and ductilely deformed feldspar and Qtz aggregates define a (D2) lineation in granitic–pegmatitic orthogneiss.

Most of the coarse-grained Qtz displays deformation bands, strong undulose extinction, migrative recrystallization of deformation bands or a restricted dynamic recrystallization along deformation band boundaries. The dynamic recrystallization is microscopically stronger in the feldspar aggregate. Pl1 and Kfs1 porphyroclasts are surrounded by a Pl2–Kfs2 grain matrix separated in layers from elongated Qtz ribbons. Large flakes of Ms–Phe1 are partly replaced by fine-grained recrystallized aggregate of the Ms–Phe2 in discrete *C*-planes (Fig. 5e). Asymmetric 'mica-fish' structures of Ms–Phe in granitic orthogneisses again confirm a general top-to-SSE extensional sliding during the D2 stage.

Originally, the large vein-type Qtz grains were separated by the Fsp coarse-grained aggregates in pegmatite. Qtz was stretched into longitudinal deformation bands forming elongated ribbons (1). Medium size (1000–1500 μm long) secondary ribbons (2) formed because of the development of oblique deformation bands within the older ribbons (1). Migration of ribbon boundaries in several directions, but preferably perpendicular to former ribbons (1, 2) caused development of a newly-formed Qtz (3) aggregate of mostly equidimensional grains (200–800, but mainly 400–600 μm).

Feldspar layers contain 0.5–8 mm size mantled porphyroclasts of Pl1 and Kfs1. Mainly δ-type but also σ-type mantled porphyroclasts are present in discrete *S–C* domains. Dynamic recrystallization of feldspars1 formed fine-grained 40–200 μm (with an average of about 100 μm) aggregates of Pl2 and Kfs2 (Fig. 5f). Some layers are even more fine-grained (50 μm). Internal parts of large quartz ribbons are recrystallized into an aggregate of 50–100 μm grains, indicating that Qtz was also a strain accommodating mineral. This is only observable in EBS images.

4.3. Impure marbles with quartz lenses

Calc–silicate rocks (Cal–Hbl–Pl–Bt–Ep–Czo–Grt–Cpx–Scp mineral assemblage) are medium-grained, in places with intrafolial folds of the metamorphic foliation. Some rocks are Fo(?)–Spl–Phl–Grt–Dol–Cal marbles with strong serpentinization of Fo(?) to Atg. A retrograde amphibolization of Di-rich Cpx is characteristic too. The microfabrics were studied in both monomineralic calcite- and two-mineralic calcite–quartz aggregates (Fig. 6a and b).

The calcite marbles are medium-grained (200–600 μm), although a 300–500 μm average predominates. Mosaic grains have lobate migrative boundaries but show unified e-lamellae fabrics. The width of such twins indicates medium-*T* conditions (scale used after Ferrill (1991)). Discrete *C*-planes are accompanied by a 'necklace' of very fine grains (40–80 μm, with a 50–60 μm prevailing grain size) due to dynamic recrystallization.

4.4. Mylonitic granite–gneiss ('Grobgneis')

The mylonitic gneiss known as 'Grobgneis' belongs to footwall of the SSC and reveals a top-to-WSW extensional shearing (D3) with a perfect ductility of Qtz and a semi-ductility of feldspars. Relic magmatic minerals (porphyroclasts of Qtz, Ms, Bt, Pl, Kfs) of a low-grade granite–mylonite are surrounded by metamorphic/mylonitic matrix (Qtz, Ms–Phe2, Bt2, Chl, Ab, ±Ep, partly recrystallized feldspars or mantled by Kfs2 and Pl2).

The microstructure (Fig. 6c) shows migrative deformation band boundaries producing oblique or asymmetric minor grains (10–20 or 20–40 μm in size) within the deformed Qtz layers enclosing the mechanically resistant feldspar porphyroclasts.

5. Recrystallization *P–T* path related to deformation

The inferred continental subduction (D1) of a pre-Alpine basement fragment led to formation of a HP rock suite now exposed as the SSC. It is represented by eclogites (Fig. 4a) and Pl-bearing HP-amphibolites (Fig. 4b) in association with serpentinized Cpx–Olv–Carb meta-ultramafics,

Table 1
P–T estimates of the burial (D1) and exhumation (D2) stages of metamorphism — the metabasic rocks of the Sieggraben SC. (Pw = Powell, 1985; P = Perchuk, 1989; EG = Ellis and Green, 1979; K = Krogh, 1988)

Sample and mineral association	*T*, °C					*P*, kbar	
	Grt–Hbl		Grt–Cpx			Grt–Cpx–Pl–Qtz	
	Pw	P	EG	Pw	K	Eckert et al. (1991)	Perkins and Newton (1981)
S35b (eclogite)							
$Grt_{Mg\text{-rich inner progr. zone}}$ + Omp1 ± Hbl1 ± Pl1 (An 14%)	772 (D1)	684 (D1)	725 ± 40 (D1)	790 (D1)	688 (D1)	14.7 ± 1.9 (D1)	12.8 ± 1.5 (D1)
$Grt_{Mg\text{-rich inner progr. zone}}$ + Omp1 + Pl1 (An 14%)			751 ± 40 (D1)	774 (D1)	718 (D1)		15.4 ± 1.5 (D1)
$Grt_{Mg\text{-rich inner progr. zone}}$ + Omp1 + Pl1 (An 14%)			762 ± 40 (D1)	774 (D1)	729 (D1)	15.5 ± 1.9 (D1)	13.6 ± 1.5 (D1)
S32b (HP amphibolite with Cpx–Pl symplectites around Hbl1)							
$Grt_{Mg\text{-rich inner progr. zone}}$ + Hbl1 + (Cpx2 + Pl2 sympl.)	702 (D1)	701 (D1)					
S33b (Pl–Hbl-bearing eclogite)							
$Grt_{Mg\text{-rich inner progr. zone}}$ + Omp1 + Pl1 (An 9.7%)			686 ± 40 (D1)	781 (D1)	634 (D1)	14.7 ± 1.9 (D1)	12.7 ± 1.5 (D1)
$Grt_{Fe\text{-rich retr. zone}}$ + Hbl2 (rim around Grt)	575 (D2)	534 (D2)					
$Grt_{Mg\text{-rich inner progr. zone}}$ + Omp1 + Pl1 (An 9.7%)			735 ± 40 (D1)	777 (D1)	686 (D1)	14.9 ± 1.9 (D1)	12.9 ± 1.5 (D1)
S26c (HP amphibolite with Cpx–Pl symplectites around Hbl1)							
$Grt_{Mg\text{-rich inner progr. zone}}$ + Hbl1	726 (D1)	655 (D1)					
$Grt_{Mg\text{-rich inner progr. zone}}$ + Hbl1	792 (D1)	686 (D1)					

Ky–Grt gneisses and schists with a high-pressure association of Ky–Kfs–Ms/Phe–Qtz ± Pl, or impure marbles with low-Na Cpx (Di-rich), Grt, Hbl, Ep and Scp.

A prograde D1 burial metamorphic trend from amphibolite- to eclogite-facies can be deduced from inclusions of Hbl1 (Prg, Hs, Ed, Ts), Pl1 and Ep1 in Omp (with the maximum Jd content of 38%) and an increasing Prp and a decreasing Grs content to the outer zones of the Grt grains. Coexistence of prismatic Omp with Hbl1, Grt, Rt, Zo and varying amount of Pl points to a transition zone between HP amphibolites and eclogites after the D1 stage.

The initial stage of the D2 exhumation is fixed by textures of ductily layered eclogitic and amphibolitic mylonites indicating the inferred master detachment fault. Prismatic Omp and Zo1 (±Hbl1) underwent dynamic recrystallization into an aggregate of minor Cpx2 ($Jd_{18\text{-}31}$) + Zo2 (±Hbl2 ± Pl2) in eclogites. Similarly, prismatic Hbl1 of eclogites (Prg, Hs) and HP amphibolites (Ed, Hb, Ts) changed to an aggregate of Hbl2 (Hb + Prg + Act) + Pl2.

Outside the inferred hanging wall detachment fault the beginning stage of exhumation is recorded by symplectitic intergrowth of Cpx2 ($Jd_{13\text{-}22}$) + Pl2 in eclogites (Fig. 4a), or of Cpx ($Jd_{3\text{-}16}$) + Pl2 in HP amphibolites (Fig. 4b) replacing HP Omp or Hbl1, respectively. Prograde zonation in Grt indicates slightly increased temperature during the reactional recrystallization of HP Omp and Hbl1. However, the Jd content of newly formed Cpx is decreasing due to decompression.

Continuing *P–T* decrease during the advanced stage of the D2 exhumation is indicated by the blue-green Al-rich Ts (or Al–Prg) rim around Grt in metabasites, the Ath–Tlc rim around Opx in Mg-rich gneisses, amphibolization of Cpx and serpentinization of Fo(?) in calc–silicate marbles, and by replacement of Grt by Bt + Ky or Bt + Sil in Kfs-bearing gneisses.

The LT-period of the D2 event is reflected by stability of Qtz, Ser–Ms/Phe, Chl, Ab, Tur in gneisses and micaschists, or by Qtz, Chl, Act, Ep, Ab, Bt, Cal in amphibolites, although the latter are of minor significance in the SSC. The attainment of equilibrium along the retrograde path is strongly dependent on fluid availibility (Rubie, 1990) and consequently high-grade assemblages may well be preserved under relatively dry conditions and rapid exhumation, as was probably the case for the SSC.

Temperature of D1 was calculated by the Grt–Cpx and Grt–Hbl thermometer using unzoned Omp or Hbl1 and contacting Grt (Mg-rich inner prograde zone). The mean values are 732 ± 30°C (Ellis and Green, 1979),

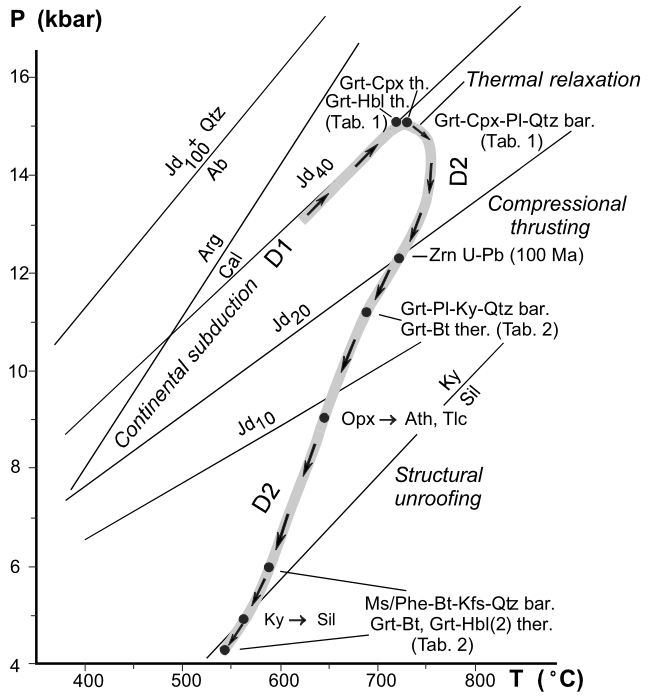

Fig. 7. Estimated P–T path of the Sieggraben eclogite-bearing structural complex using the data from Tables 1 and 2 for the D1 and D2 deformation stages. Further explanation in text.

779 ± 11°C (Powell, 1985), and 691 ± 38°C (Krogh, 1988) (Table 1). The maximum temperature close to the pressure peak of metamorphism (D1) may be considered to be 700–750°C (734 ± 40°C is the mean value of the Grt–Cpx thermometers used). For comparison, a mean T of 748 ± 44°C was estimated using Grt–Hbl(1) thermometry after Powell (1985), and 682 ± 30°C after Perchuk (1989). The value of 748–682 is quite compatible with results of the Grt–Cpx thermometry.

Pressure was estimated according to Grt–Cpx–Pl–Qtz geobarometers of Perkins and Newton (1981) at (P_{mean}) 13.5 ± 1.8 kb, and Eckert et al. (1991) at 15 ± 0.3 kb (Table 1). According to Jd_{38} isopleth in Omp at 720°C (Holland, 1980) the P value is 15 kb (Fig. 7). So, the maximum pressure (D1) may be considered to be about 15 kbar.

Missing, or at least indistinct, direct contacts of Grt with Cpx2 grains from Cpx2–Pl2 symplectites around Omp or Hbl1 do not permit the use of Grt–Cpx thermometers to prove the assumed increasing T during the initial stage of the D2 exhumation. The stage of formation of Hbl2 (±Pl2) kelyphitic rims around Grt (with narrow outer retrograde rim) was estimated according to Grt–Hbl thermometry at 534–575°C (Table 1).

Grt–Bt thermometry (Perchuk, 1989) in gneisses revealed 675 ± 25°C at higher pressures of 11.5 ± 1.5 kbar (Grt–Ky–Pl–Qtz barometry, according to Koziol (1989); Table 2) or 530–600 ± 30°C at estimated pressures lower than 7 kbar (using phengite barometry on Ms–Phe, according to Massonne and Schreyer (1987)) of the D2 exhumation (Table 2).

The steep part of the P–T path (Fig. 7) is probably related to a rapid (compressional?) early D2 exhumation following the thermal relaxation. Next, a more equivalent decrease of P and T is interpreted to indicate the late D2 stage or SSE-ward extensional structural unroofing (structural denudation) of the SSC along a detachment fault zone.

6. Deformation mechanisms and mineral CPO patterns of mylonites

6.1. Omphacite, hornblende and zoisite in eclogite–mylonites

The eclogites show distinct (NNW–SSE) mineral lineations defined by shape preferred orientation of Omp (N_Z

Table 2
Pressure estimates of the D2 stage of metamorphism according to Grt–Pl–Ky–Qtz barometer (Koziol, 1989) and the Phe–Bt–Kfs–Qtz barometer (Massonne and Schreyer, 1987) for paragneisses (S28, S37b, S37II) and metaganites (S19c, S21). The temperature was calculated using the Grt–Bt thermometer (Perchuk, 1989)

Sample	Mineral assemblage	Si content in the analyzed Ms–Phe (p.f.u.)	T (°C), Grt–Bt thermometry for Grt_{rim}–Bt pairs (Perchuk, 1989)	P (kbar)	
				Ms–Phe–Bt–Kfs–Qtz barometry (Massonne and Schreyer, 1987)	Grt–Pl–Ky–Qtz barometery (Koziol, 1989)
S28	Ms–Phe–Bt–Grt–Ky–Kfs–Pl–Ilm–Qtz	–	675 ± 30 (D2)	–	11.5 ± 1.5 (D2)
		3.21	Values for a retrograde path: 600–530 (D2)	6.5 ± 0.5	
S19c	Ms–Phe–Bt–Pl–Kfs–Qtz	3.17–3.20		5.5 ± 0.5	
S21	Ms–Phe–Bt–Pl–Kfs–Qtz	3.11–3.22		4.5 ± 1.5	
S37b	Ms–Phe–Bt–Tur–Pl–Kfs–Qtz–Ep	3.11–3.16		4.0 ± 1.0	
S37II	Ms–Phe–Bt–Tur–Pl–Kfs–Qtz	3.14–3.16		5.25 ± 0.25	

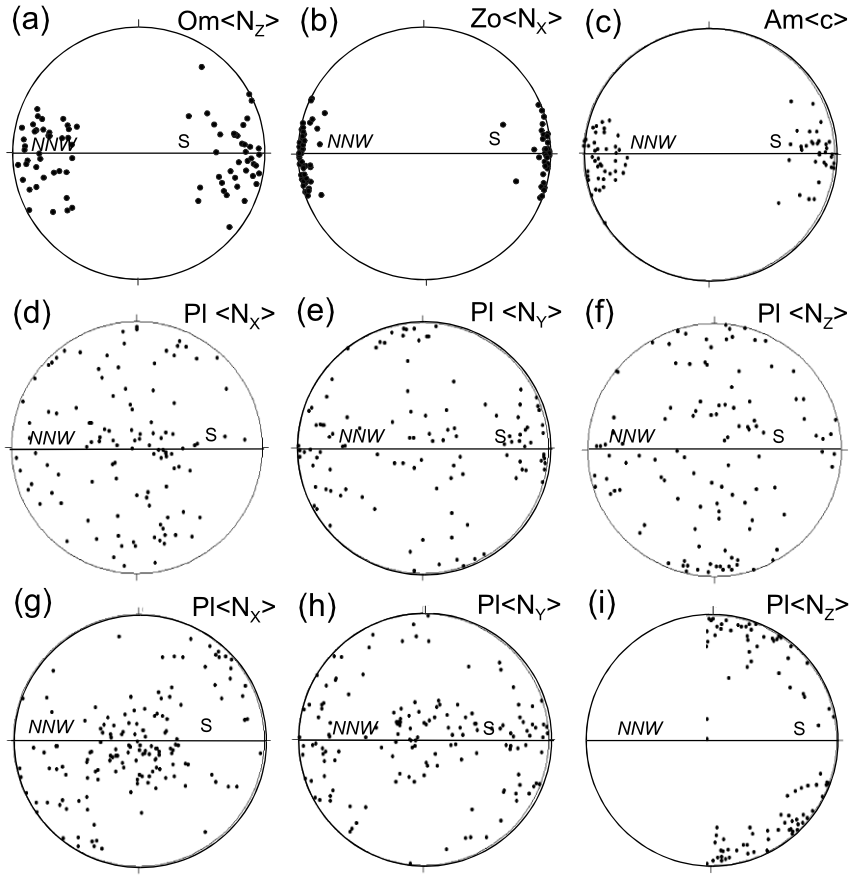

Fig. 8. The U-stage microscope patterns of Omp, Zo1, Hbl1 and Pl2 (Sieggraben SC). *XZ* section parallel to lineation and perpendicular to foliation. (a) D1 Omp (S35, $N = 80$), eclogite. (b) D1 Zo1 (S35, $N = 90$), eclogite. (c) D1 Hbl1 in Grt amphibolite–mylonite (S32, $N = 78$). (d–f) D2 Pl2 in layered amphibolite (S8, $N_{d-f} = 113$). (g–i) D2 Pl2 in granitic orthogneiss (S1, $N_{g-i} = 151$) indicating (010) [001] slip operative in Pl.

optical direction, Fig. 8a), Zo1 (N_X, Fig. 8b) and a smaller amount of Hb1 (⟨c⟩, Fig. 8c) prismatic crystals measured by U-stage. A linear preferred orientation fabric of prismatic Omp, Zo1, ±Hbl1 associated with Grt and Rt in the foliation of eclogites developed by oriented mineral metamorphic growth during progressive (D1) burial (continental subduction).

Omp porphyroclasts (Fig. 5a) mantled by dynamically recrystallized equidimensional mostly omphacitic Cpx2 new grains indicate a progressive deformation (D2 exhumation) accommodated by dislocation creep and a dominant rotation–recrystallization mechanism in the highly strained layers (Philippot and van Roemund, 1992). Generation of a well-defined 'subgrain' structure is thought to be a reliable indicator of dislocation creep at temperatures between 500 and 600°C (Godard and van Roemund, 1995).

In the studied eclogites of the SSC dynamic recrystallization of Cpx1 (Omp), in the inferred hanging wall domain, was initiated at about 750°C after thermal relaxation. Later, dynamic recrystallization was simultaneous with high-temperature reaction recrystallization or the breakdown of Omp in the low-strain domain at ca. 700–650°C and 12–9 kbar (Fig. 7).

6.2. Horblende, plagioclase and quartz in HP amphibolite–mylonites

Hbl1 exhibits a pronounced shape-preferred orientation with [001] indicating a strong mineral lineation observable in foliation planes. The crystallographic preferred orientation of hornblende was formed during prograde metamorphic growth (D1 burial) and was determined by individual grain measurements using a U-stage (Fig. 8c).

The superimposed plastic deformation and recrystallization of the Hbl1 is indicated by the microstructure. Slip on (100) planes parallel to the *c*-axis produced twins parallel to Hbl prism planes and kinking of prismatic (110) planes. Deformation (100) twins, bending and undulose extinction along {100} planes, crosscutting kink bands, tension gashes, microfaults and book-shelf structures of Hbl1 point to ductile and later ductile/brittle deformation of Hbl1 during the progressive (D2 exhumation) deformation.

Many twinned Pl1 grains, especially in layered amphibolite–mylonites display subparallel orientation of twins with the foliation planes. The type (010 or 001) and orientation of twins as well as optical directions oriented at low angles to their normals were measured by a U-stage (Fig. 8d–f).

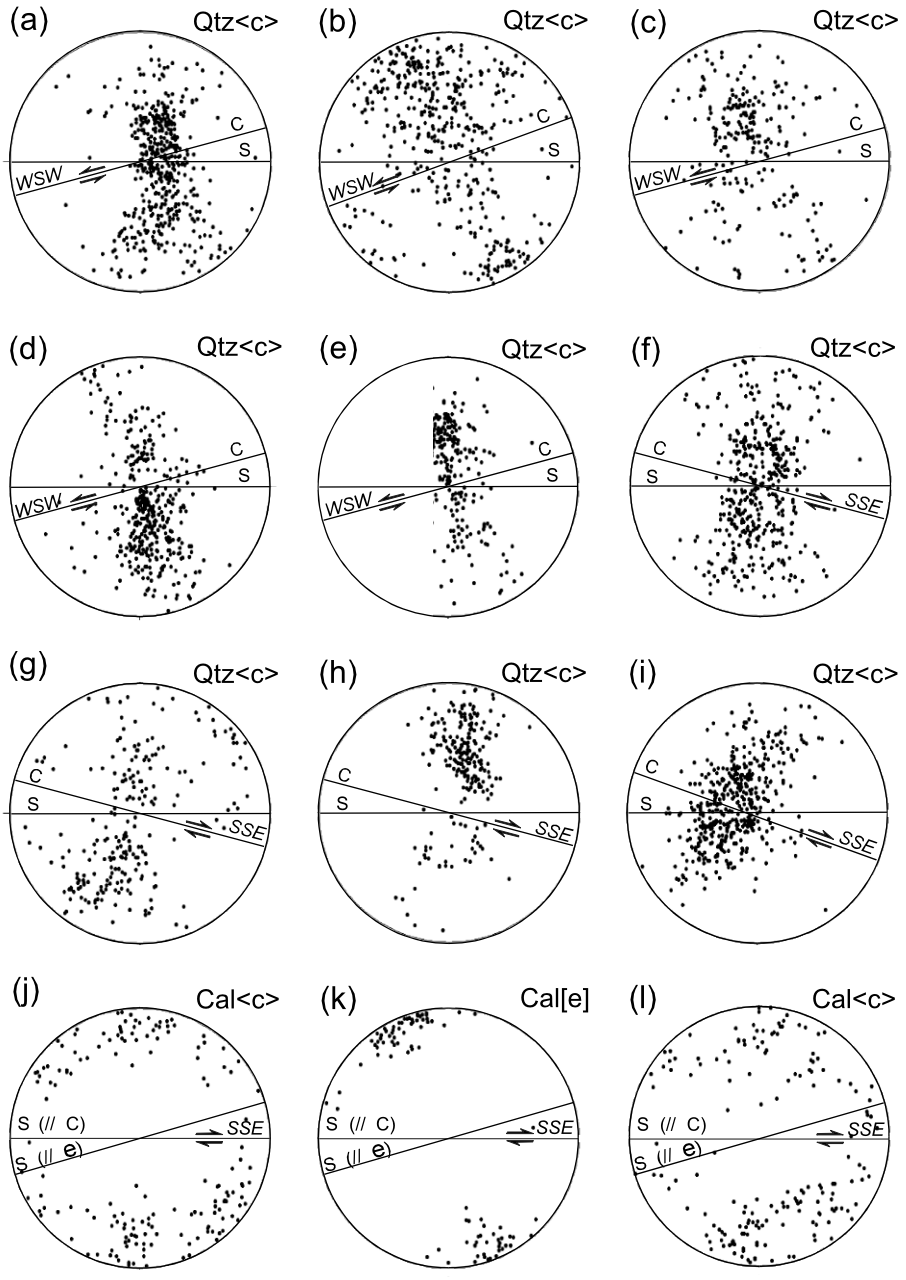

Fig. 9. The U-stage microscope patterns of Qtz and Cal. Qtz *c*-axes (a–i), Cal *c*-axes (j, l) and Cal e-poles (k) preferred orientation patterns. 'Grobgneis' structural complex (a–e, D3). Sieggraben structural complex (f–l, D2), *XZ* sections: (a, d, e) 'Grobgneis' granitic mylonite (a — G3, $N = 456$; d — G13a, $N = 403$; e — G13b, $N = 331$). (b) Paragneiss mylonite (G4, $N = 431$). (c) Metaconglomerate–mylonite (G5, $N = 228$). (f) Layered amphibolite (S8, $N = 421$). (g, i) Granitic orthogneiss–mylonite (g — S2, $N = 229$; i — S1, $N = 461$). (h) Quartz layer in marble mylonite (S107, $N = 229$). (j–l) Marble (j — S11, $N = 167$; k — S11, $N = 89$; l — S11, $N = 176$).

The presence of mantled to entirely dynamically recrystallized Hbl1 and Pl1 and of mixed Hbl2–Pl2 aggregates suggest dislocation creep as an active deformation mechanism (Tullis and Yund, 1985; Hacker and Christie, 1990) and accommodation by subgrain rotation as the principal process of recrystallization. The sigmoidal-plastic shaped (Fig. 5c and d) Hbl1 porphyroclasts show recrystallization into sodic–calcic Prg–Hbl2 in the high-strain- or higher-Al Prg–Hbl2 in the low-strain domains at high temperatures, or low-Al Hbl2 to Act–Hbl2 at medium temperatures.

Some of the mechanically separated Pl-rich layers are characterized by extremely fine-grained ultramylonitic Pl2 grains (Fig. 5c and d). Grain boundary sliding or superplastic flow (Bouillier and Gueguen, 1975) might contribute to ductile weakening in such extremely fine grained bands of Pl2.

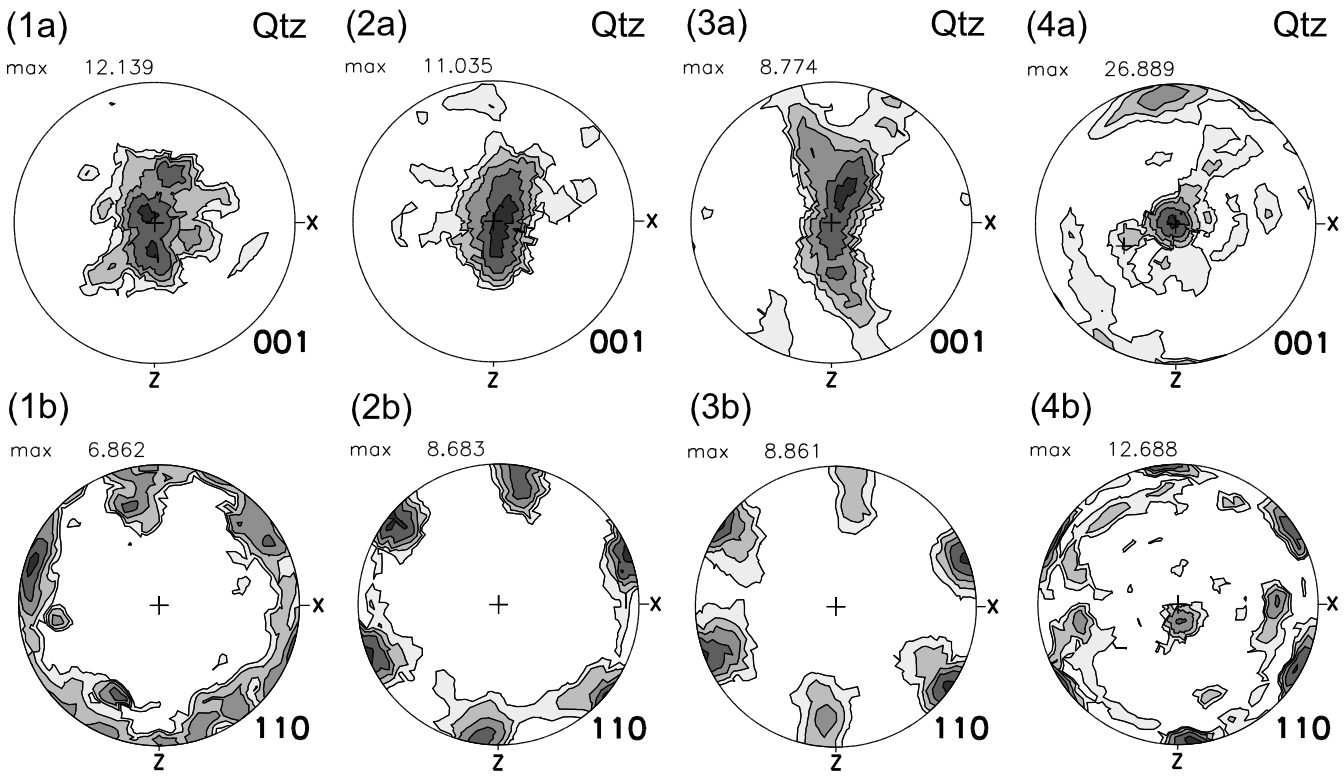

Fig. 10. The X-ray texture goniometer patterns of Qtz (Sieggraben SC 1–2, Grobgneis SC 3–4). (1a, b) Prism ⟨a⟩ and a rhomb (D2) slip dominated in Qtz of mylonitic granite–gneiss (s. S1). (2a, b) Prism ⟨a⟩ and a rhomb dominated slip (D2) in Qtz of quartz layer in marble (s. S107). (3a, b) Prism ⟨a⟩, rhomb and basal ⟨a⟩ slip in Qtz (D3) of quartz layer in mylonitic paragneiss (s. G4). (4a, b) Prism ⟨a⟩ and basal ⟨a⟩ slip with contribution of a rhomb slip (D3) in Qtz of Grobgneis type mylonitic orthogneiss (s. G3).

It was possible to measure the minor grains of Pl2 (with 10–16% An content), a product of dynamic recrystallization of Pl1 (with 9–16% An content) in the light-coloured bands of amphibolite by U-stage. The orientation of N_X (Fig. 8d), N_Y (Fig. 8e) and N_Z (Fig. 8f) optical directions indicate a slip activity on {010} planes close to the foliation in the direction of [001] or N_Y subparallel to lineation. Although most of the N_Z (or γ) optical directions are subparallel to the Z-axis of finite strain, some of them are subparallel to the lineation, thus suggesting slip activity on {001} planes. This is also valid for N_Y (or β). Nearly symmetric pattern distribution of measured optical directions, and taking into account an acute crystallographic angle between the optical (N_Z) and [010] poles, an almost pure-shear deformation regime in relation to the foliation and lineation can be envisaged. This type of pattern and slip system is generally reported for high-grade (amphibolite- to granulite facies) mylonites (Olsen and Kohlstedt, 1985; Ji and Mainprice, 1990; Egydio-Silva and Mainprice, 1999).

Prism ⟨a⟩ slip with a contribution of rhomb slip (Lister and Hobbs, 1980; Schmid and Casey, 1986) apparently dominated in Qtz present in the light-coloured bands of amphibolite–mylonites (Fig. 9f). It is consistent with two distinct concentrations of c-axis poles: in the middle of the diagram, and at a medium distance from the center of the pattern.

6.3. Quartz, feldspars and white mica in mylonitic granite–gneisses

Quartz ribbons (Wilson, 1975; Culshaw and Fyson, 1984) in mylonitic gneisses may characterize relatively higher-temperature fabrics. In the low shear strain domains, the boundaries of longitudinal deformation bands (1) in the original coarse-grained Qtz of a granitic pegmatite migrated preferably in the direction of plastic flow during prograde metamorphism (D1 burial) producing elongated ribbons (1). However, the boundaries of oblique internal deformation bands (2) migrated at high angles to the direction of flow (or to prolongation of ribbons (1)), producing sutured almost equidimensional Qtz grains (3) (Fig. 5e). The new grains (3) have a very pronounced CPO fabric that seems to be the product of both migration recrystallization (bulge nucleation) and subgrain lattice rotation mechanisms (Gleason and Tullis, 1993; Trimby et al., 1998).

The Qtz ribbons grew until increasing shear strain initiated both the grain-boundary migration recrystallization (recognized by sutured grain boundaries) and progressive subgrain rotation (indicated by the measured CPO patterns). The process of subgrain formation is only observable in EBS images along deformation band boundaries or within 'homogeneous' ribbon domains. There are still abundant low-angle boundaries within the optically 'homogeneous'

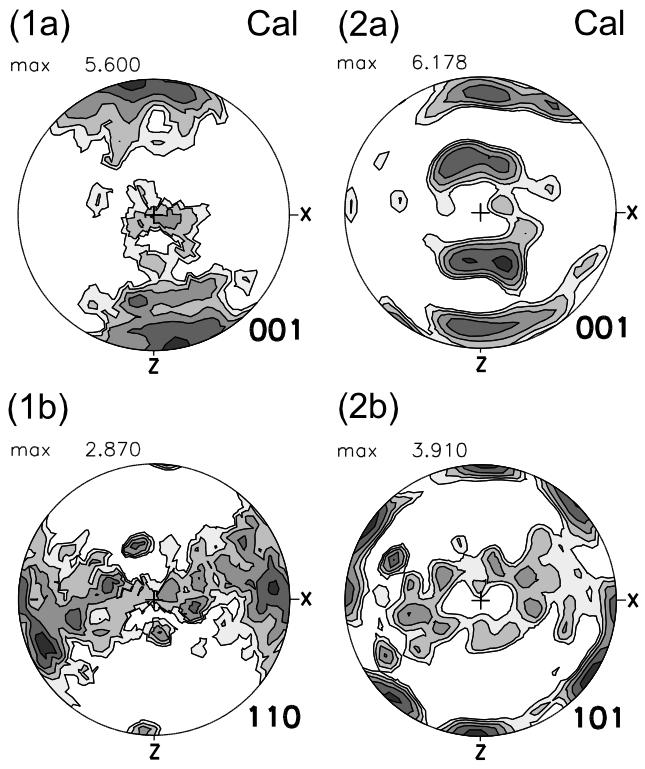

Fig. 11. The X-ray texture goniometer patterns of Cal (Sieggraben SC). (1–2) Cal fabrics (late D2) in mylonitic marble (1a, b — s. S107, 2a, b — s. S34).

ribbons. The subgrain microstructure suggests that recovery influenced the development of these microstructures. The subgrains orientation was initially close to the parent band, but some grains indicate a progressive misorientation (with distinct angles of extinction) or new high-angle boundaries due to subgrain rotation. The subgrains of Qtz have indistinct (relatively low-angle) boundaries compared with those in the adjacent feldspar layers.

Migration recrystallization of Qtz ribbons forming internal subgrains to real new grains in the process of dynamic recrystallization (Urai et al., 1986; Knipe and Law, 1987; Drury and Urai, 1990) seems to be contemporaneous with the process of dislocation creep (Hirth and Tullis, 1992) which took place predominantly by prism ⟨a⟩ and rhomb slip in Qtz ribbon grains (3) according to preferred orientation patterns obtained by U-stage (Fig. 9i) and X-ray texture goniometer (Fig. 10/1a and 1b). The recurrent typical medium-*T* textural patterns of Qtz are overprinted by lower-*T* ones in the hanging wall thrust plane of the SSC that accumulated the subsequent reactivation. This is reflected by operative basal ⟨a⟩ slip (Fig. 9g).

The feldspar layers (Fig. 5e and f) consist of equidimensional Pl(2) and Kfs(2) grains with arcuate to straight boundaries meeting at 120° triple junctions, suggesting late kinematic annealing related to D2 extensional exhumation. Some relic lobate or sutured grain boundaries might indicate the former strain-induced grain boundary migration (bulge nucleation), followed by subgrain rotation (Poirier and Guillopé, 1978; Jensen and Starkey, 1985). Evidence for subgrain rotation recrystallization is illustrated by the presence of a core and mantle structure within original feldspar grains (Fig. 5e). The higher-temperature process of dynamic recrystallization is also documented by a higher content of Ab in Kfs2 (5.1–8.2%). Rare undulatory white mica (Ms–Phe) 'fishes' are dynamically recrystallized along their margins (Fig. 5e).

Pl(2) preferred orientation of N_X (Fig. 8g), N_Y (Fig. 8h) and N_Z (Fig. 8i) optical directions, especially those of N_Z located at high angle to foliation, indicate dislocation creep in {010} [001] slip system in Pl (with 10–16% An content).

6.4. Quartz lenses in calcite marble mylonites

The microstructures of Qtz lenses and bands within the mechanically twinned calcitic matrix of marble mylonites show migration recrystallization into ribbons (1) and oblique smaller ribbons (2) within the host ribbons (1) during the medium-*T* period of the D2 extensional deformation.

Qtz layers in marbles show low-*T* dynamic bulging to polygonization (Fig. 6a), but this is restricted to discrete boundary zones of still well preserved medium-*T* Qtz ribbons. With increasing strain and decreasing temperature the lattice in the bulges becomes progressively misoriented from the adjacent host ribbon grains.

The Qtz *c*-axes pole figure (Fig. 9h) reflects dislocation creep in rhomb and basal ⟨a⟩ slip systems. The pattern also comprises the orientations of polygonal grains located along the ribbon boundaries (Fig. 6a) with the dominating basal slip.

The X-ray texture goniometer pattern of Qtz *c*-axes (Fig. 10/2a and 2b) exhibits a prolonged central Y-maximum as the result of dominated medium temperature prism ⟨a⟩ slip combined with a rhomb one in an almost pure shear deformation regime. This pattern reflects the bulk Qtz orientation or still predominating higher-temperature fabric of ribbons and their internal grains.

The Qtz texture appears to be simultaneous with the development of quite unified Cal e-lamellae fabrics in the host marble mylonite. Cal e-lamellae indicate medium- to low-temperature mechanical twinning (according to width of lamellae; Ferrill, 1991), which is easier in coarse-grained marbles, enhancing strain weakening. The X-ray texture goniometer patterns of such deformed marbles reflect a top-to-SSE simple shear (Fig. 11/1a and 1b) supported by a basal ⟨a⟩ and r-slip in Cal (Nicolas and Poirier, 1976).

6.5. Calcite in marble mylonites

Calcite grains in marble mylonite (Fig. 6b) show an internal medium- to low-temperature e-lamellae fabric (Ferrill, 1991) parallel to flattened individual grains that is oblique to the *C*-planes marked by dynamically recrystallized Cal(2) grains within discrete shear bands. This is in

agreement with simple shear experiments in the twinning regime if a single dominant twin orientation is observed, and the non-recrystallized original grains define a grain shape fabric that is oblique to the shear zone boundaries. The twinned grains preserve lobated grain boundaries, which are assumed to represent the higher-temperature grain boundary migration that transformed at higher strains and differential stresses to mechanical twinning (regime 1, Schmid et al., 1980). Later on minor subgrains and recrystallized grains along the shear (*C*) foliation form, indicating new strain localization, probably at a lower temperature and higher deformation rate.

Calcite e-poles (Fig. 9k) and *c*-axes (Fig. 9j and l) indicate the position of the shortening tectonic axis *x* that acted almost subvertically during the Early Cretaceous (late D2) exhumation period connected with the top-to-SSE extension shearing of the MAA basement. A pure shear (Fig. 11/2a and 2b) deformation regime was found in the e-lamellae fabrics too.

6.6. Quartz and feldspars in mylonitic granite–gneiss ('Grobgneis')

The Qtz layers are recrystallized into an aggregate of obliquely oriented short micro-grains (Fig. 6c). The asymmetry is consistent with the overall top-to-SW low-temperature extensional *S–C* type mesostructures. The asymmetric Qtz *c*-axes patterns measured by U-stage are the result of combined prism ⟨a⟩, rhomb and basal ⟨a⟩ slips (Fig. 9a–e). They are consistent with *S–C* fabrics and top-to-WSW shearing during the D3 exhumation. The texture goniometer patterns (Fig. 10/3a and 3b–4a and 4b) suggest that medium temperature prism ⟨a⟩ slip dominated, with a contribution of rhomb and basal ⟨a⟩ slips in an approximately pure shear regime. Feldspar deformation indicates an initiation of mantle subgrain formation (Fig. 6c). Most of Kfs or Pl porphyroclasts shows healed tension gashes to fractures.

7. Discussion

7.1. Paleotectonics, timing and metamorphic conditions of Alpine eclogites

Comprehensive reviews of eclogite-facies rocks in the Alps have been provided by Droop et al. (1990), Dal Piaz et al. (1993), Oberhänsli (1994), Froitzheim et al. (1996), Spalla et al. (1996) and Dal Piaz (1999). The Cretaceous orogeny in the internides of the Eastern Alps occurred due to collision between the Austro–Alpine (AA) continental crust (include the central Western Carpathians) and a continent in the southeast (pre-Tissia, Fig. 1) after closure of the Middle Triassic–Early Jurassic Meliata–Hallstatt oceanic basin (Fig. 2) in the Middle to Late Jurassic (at ca. 150 Ma; Dallmeyer et al., 1996). However, the AA eclogites do not represent this suture zone with maximum blueschist-facies HP rocks (Faryad, 1997), but suggest a shortening and continental subduction of some thinned AA basement fragments within the passive continental margin of the Meliata–Hallstatt basin (Neubauer, 1994; Froitzheim et al., 1996; Putiš et al., 2000). This new interpretation of the Early Alpine evolution of the Eastern Alps comes from the Western Carpathians, notably the Meliata(–Hallstatt) Ocean remnants and the Meliata Nappe (Kozur and Mock 1973; Kozur, 1991). Subduction of the Meliata unit oceanic crust took place in the Middle- to Late Jurassic and the subsequent (Cimmerian) shortening of the adjacent (Veporic–Gemeric) passive continental margin (Putiš, 1991; Plašienka et al., 1997) was constrained at ca. 110–85 Ma (Dallmeyer et al., 1996).

Radiometric data suggest an Early Cretaceous age (around 100 Ma) of the eclogite-facies metamorphism in the Eastern Alps, including the Sieggraben eclogites (Dallmeyer et al., 1992; Thöni and Jagoutz, 1993; Putiš et al., 2000). The so-called Middle AA unit (Tollmann, 1977) is the only unit containing Early Cretaceous eclogites. The Lower AA unit underwent Early Cretaceous LT/(MT)–MP/(HP) metamorphism too (Korikovsky et al., 1998), while the Upper AA unit escaped from the continental subduction zone and was stacked over the thickened continental collisional wedge (Platt, 1993) like an orogenic 'lid'. Such a general structure indicates a suture after the closure of the Meliata–Hallstatt ocean that is inferred to be located in space between the root zone of the Upper AA unit and the Southern Alps (Fig. 2). The continental underthrusting (subduction, underplating) zone that included (HP–MP) part of the Lower AA unit, the main (HP) part of the Middle AA unit (with the Sieggraben eclogites) can therefore be inferred in the area between the Upper AA unit root zone and the northern margin of the AA unit (Fig. 2). The proposed paleotectonic scheme and recognized Early Cretaceous collision structure is also applicable eastwards for the central Western Carpathians (north of the Meliata Nappe suture), where the Veporic unit underwent continental collisional underthrusting and metamorphism in the maximum lower amphibolite facies conditions (ca. 520°C at 7–9 kbar; Putiš et al., 1997a). It was overthrust by the Gemeric unit with the basement/cover complexes resembling the Upper AA and Southern Alps units.

For a comparison, an eclogite-facies metamorphism in the Pennine Tauern Window of the Eastern Alps seems to be clearly diachronous — Early Tertiary (at ca. 60–45 Ma, according to Zimmermann et al. (1994) and Kurz and Neubauer (1998)) and indicates a younger collision due to closure of the Pennine oceanic basin. The tectonic regime of eclogitization is related to approximately N–S (to NW–SE) compression between the amalgamated AA–South Alpine (Apulian) and European plates (Fig. 2).

Some of colliding thinned AA basement fragments, metamorphosed in HP amphibolite- to eclogite-facies (the Polinik unit in the Kreuzeck Massif, after Hoke, 1990) south of the Tauern Window show Latest Cretaceous–Early

Table 3
Deformation mechanisms and slip systems of strain accommodating minerals during the D2 and D3 exhumation stages

Sample	Rock type	Strain accom. phases	Dynam. recr. phases	Dynamic recryst. type	Active slip system	*T*/*P* (°C/kbar)	Def. regime
Zöb1	Eclogite	Cpx1 (Omp) (Jd32-38)	Cpx2 (Jd18-31)	Rotation	Not found	750–650/15–9	D2 exhumation
S22	HP amphibolite	Hbl1	Hbl2	Rotation	Not found	700–500/12–3.5	D2 exhumation
S22	HP amphibolite	Pl1	Pl2 (<10 (m)	Superplast. flow?	GBS	700–500/12–3.5	D2 exhumation
S8	HP amphibolite	Pl1	Pl2	Rotation	(010) [001]	700–500/12–3.5	D2 exhumation
S8	HP amphibolite	Qtz ribbons	Qtz grains	Migration + rotation	Prism ⟨a⟩ + rhomb	600–500/8–3.5	D2 exhumation
S1	Granitic orthogneiss	Pl1 (+Kfs1)	Pl2 (+Kfs2)	Rotation	(010) [001]	700–500/12–3.5	D2 exhumation
S1	Granitic orthogneiss	Qtz ribbons	Qtz subgrains	Dynamic recovery	–	700–500/12–3.5	D2 exhumation
S1	Granitic orthogneiss	Qtz ribbons	Qtz grains	Migration + rotation	Prism ⟨a⟩ + rhomb	600–500/8–3.5	D2 exhumation
S107	Qtz lense in marble	Qtz ribbons	Qtz grains	Migration + rotation	Prism ⟨a⟩ + rhomb	600–500/8–3.5	D2 exhumation
S107	Qtz lense in marble	Qtz ribbons	Shear band Qtz	Rotation	Rhomb + basal ⟨a⟩	500–300/<3.5	D2 exhumation
S107	Marble	Cal1	Cal2 grains	Rotation	Basal + r	500–300/<3.5	D2 exhumation
S11	Marble	Cal1	Cal1 twins	Mechanic twinning	e	500–300/<3.5	D2 exhumation
S34	Marble	Cal1	Shear band Cal2	Rotation	Basal + r	500–300/<3.5	D2 exhumation
G3	Grobgneis granitic orthogneiss	Qtz bands	Oblique Qtz grains	Migration + rotation	Prism ⟨a⟩ + rhomb + basal ⟨a⟩	500–300/<3.5	D3 exhumation
G4	Paragneiss	Qtz bands	Oblique Qtz grains	Migration + rotation	Prism ⟨a⟩ + basal ⟨a⟩ ± rhomb	500–300/<3.5	D3 exhumation

Tertiary (ca. 70–50 Ma cooling ages; Oxburg et al., 1966) exhumation in dextral strike-slip suture zone (Putiš et al., 1997b, 1998). The age of their HP metamorphism has not yet been constrained.

In the Western Alps, during the Latest Cretaceous and Early Tertiary (ca. 70–40 Ma), Pennine oceanic lithosphere (at ca. 50–40 Ma) together with the thinned Pennine continental basement slivers (Brianconnais, at ca. 40 Ma) and part of Sesia continental ribbon (SCR at ca. 70–60 Ma) were subducted under the Apulian margin, now represented here by the Southern Alps along the Periadriatic (or local Canavese) tectonic boundary line. The SCR is an extensional allochthon separated from the AA margin by riftogenous detachment faulting, according to Froitzheim et al. (1996). From this point of view, a shortened AA continental margin, with the Early Cretaceous eclogites, is lacking in the western and central part of the Alps. Even if one considers the Sesia and some other continental fragments of the inner Pennine domain to be structurally part of the AA unit (Spalla et al., 1996; Dal Piaz, 1999; and others), the timing of HP metamorphism is different from the same event in the Eastern Alps. The tectonic regime of eclogitization is inferred to be related to approximately E–W (to WNW–ESE) compression between the Apulian (Adriatic) and European plates during the dextral strike slip or westwards shifting of the AA–South Alpine (Apulian) segment, colliding with the Pennine structural complexes in the Western Alps.

The *peak P–T* conditions of the Early Cretaceous Eastern AA continental eclogite-bearing units reached 14–16 kbar at 600–700°C and was followed by thermal relaxation to almost 800°C (Neubauer et al., 1992; Putiš et al., 1998, 2000). The Western AA (?) or continental Pennine (?) Sesia and the other intra-Pennine continental fragments usually reached 15–20 kbar at 500–600°C (reviewed by Spalla et al., 1996; Dal Piaz, 1999), which is consistent with the HP metamorphism of adjacent Mesozoic ophiolites (Ring, 1992). Some of these (e.g. the Dora Maira continental fragment) show Eocene–Oligocene HP–UHP metamorphic depths (Gebauer et al., 1993; Duchéne et al., 1997).

7.2. The Sieggraben eclogites of the Eastern Alps

The strain episodes (D1–D3) that we have distinguished and the inferred micromechanisms of ductile deformation and dynamic recrystallization give information on the hanging wall master detachment fault responsible for the exhumation of the eclogite-bearing Sieggraben structural complex (SSC).

Internal or weakly-sheared domains of the eclogitized SSC complex were subjected to predominating reaction recrystallization that reflect temperature and pressure changes during burial (D1 stage) and exhumation (D2 stage). Thus, HP minerals such as Omp (Cpx1) and Hbl1 are partly substituted by HP–MP/HT Cpx2–Pl2 symplectites.

The main micromechanism of ductile deformation in the strongly-sheared domains seems to be dislocation creep connected with dynamic recrystallization of strain accommodating minerals (Table 3). Plastic deformation of Omp slightly predated plastic deformation of Hbl(1) and Pl(1) at high temperatures (750–650°C), because some of the Omp porphyroclasts are fractured within ductile Hbl2–Pl2 aggregate. The plasticity of Hbl and Pl continued at medium temperatures (650–500°C) in metabasites. Feldspars and Qtz were plastically deformed and recrystallized at medium temperatures in granitic orthogneiss. The high-temperature Qtz ribbons are partly replaced by equant grains due to combined dynamic migration–rotation recrystallization with the crystal–plastic deformation by prism ⟨a⟩ and a rhomb slip at medium-temperature (D2 exhumation stage). Cal in marble was preferably deformed by mechanical twinning, while Qtz ribbons in separated Qtz layers were intensively recrystallized along discrete shear bands. However, the Qtz layers in Grobgneis-type orthogneiss and adjacent paragneiss–mylonites (D3 exhumation stage) show more complicated textural patterns as the result of prism ⟨a⟩, a rhomb and basal ⟨a⟩ slips at an estimated temperature of 500–300°C.

The measured textural patterns are coeval with mesoscopic kinematic indicators for top-to-SSE extensional sliding during D2 exhumation by the inferred mechanism of structural unroofing (structural denudation). A superimposed, top-to-WSW extensional shearing represents a younger low-temperature exhumation (D3) event that overprints the base of the studied eclogitic complex. It is compatible with the structures recognized in the footwall LAA Grobgneis and Wechsel structural complexes.

The microstructures and textural patterns reflect the major tectonic events (D1–D3) and the mineral aggregates record superimposed deformation–recrystallization stages. Competition existed between reaction recrystallization (predominating in the low shear strain domains) and dynamic recrystallization (in the high shear strain domains); these microfabrics do not overlap in any microdomain.

The mean temperature estimates of about 720°C (using Grt–Cpx and Grt–Hbl thermometry) close to a pressure peak at ca. 15 kbar (using Grt–Cpx–Pl–Qtz barometry) suggest a depth of 50–55 km for the eclogitization process in the investigated region of the Eastern Alps.

The estimated values point to continental subduction of the studied basement fragment (SSC) at an average geothermal gradient of ca. 13°C/km (D1). The cooling rate of ca. 40°C/Ma during the exhumation D2 stage, derived from geochronological data (Putiš et al., 2000 — Zrn U–Pb data; Dallmeyer et al., 1992, 1996 — Am ^{40}Ar–^{39}Ar data), implies an exhumation rate of ca. 4–5 km/Ma.

Structural–petrological data are coeval with the proposed model of polyphase exhumation of the SSC along a master detachment fault that developed during the compressional

wedge formation (D1), through the structural denudation (unroofing, D2) and passive thrusting over the underlying Lower AA structural complexes (D3).

Acknowledgements

Research costs were covered by the Austrian Geological Survey mapping program, VEGA grant of Slovak Republic (No. 1/5228/98, 1/8248/01 M.P.), Geological Institute of K.F. University of Graz, Austria, Russian Foundation for Basic Research (project # 99-05-64058, S.P.K.). The paper benefited from research facilities at the Technical University of Denmark (Copenhagen–Lyngby) as well as research support from Villum Kann Rasmussen Fonds. We are very grateful to two referees for the constructive criticism and recommendations for the manuscript improvement. Mrs B. Wallbrecher is greatly acknowledged for correction of the English.

Appendix A. Mineral abbreviations in text and figures (after Kretz, 1983; end-members of Ca-amphiboles after Leake et al., 1997)

Ab = albite, Act = actinolite, Am = amphibole, An = anorthite, Atg = antigorite, Ath = anthophyllite, Bt = biotite, Cal = calcite, Carb = carbonate, Chl = chlorite, Czo = clinozoisite, Cpx = clinopyroxene, Di = diopside, Dol = dolomite, Ed = Edenite, Ep = epidote, Fo = forsterite, Grs = grossular, Grt = garnet, Hb = horblende, Hbl = hornblende, Hs = hastingsite, Ilm = ilmenite, Jd = jadeite, Kfs = kalifeldspar, Ky = kyanite, Ms = muscovite, Olv = olivine, Omp = omphacite, Opx = orthopyroxene, Phe = phengite, Phl = phlogopite, Pl = plagioclase, Prg = pargasite, Prp = pyrope, Qtz = quartz, Rt = rutile, Scp = scapolite, Ser = sericite, Sil = sillimanite, Spl = spinel, Ts = tschermakite, Ttn = titanite, Tlc = talc, Tur = tourmaline, Zo = zoisite.

References

Berthé, D., Choukroune, P., Jegouzo, P., 1979. Orthogneiss, mylonite and non-coaxial deformation in granites: the example of the South Armorican shear zone. Journal of Structural Geology 1, 31–42.

Bouillier, A.M., Gueguen, Y., 1975. SP-mylonites: origin of some mylonites by superplastic flow. Contributions to Mineralogy and Petrology 50, 93–104.

Culshaw, N.G., Fyson, W.K., 1984. Quartz ribbons in high grade granite gneiss: modifications of dynamically formed quartz *c*-axis preferred orientation by oriented grain growth. Journal of Structural Geology 6, 663–668.

Dallmeyer, R.D., Neubauer, F., Handler, R., Müller, W., Fritz, H., Antonitsch, W., Hermann, S., 1992. $^{40}Ar/^{39}Ar$ and Rb–Sr mineral age controls for the Pre-Alpine and Alpine tectonic evolution of the Austro–Alpine nappe complex, Eastern Alps. In: Neubauer, F. (Ed.). ALCAPA — Field Guide. University of Graz, pp. 47–59.

Dallmeyer, R.D., Neubauer, F., Handler, R., Fritz, H., Müller, W., Pana, D., Putiš, M., 1996. Tectonothermal evolution of the internal Alps and Carpathians: evidence from $^{40}Ar/^{39}Ar$ mineral and whole-rock data. Eclogae Geologicae Helvetiae 89, 203–227.

Dal Piaz, G.V., 1999. The Austroalpine–Piedmont nappe stack and the puzzle of Alpine Tethys. In: Gosso, G., Jadoul, F., Sella, M., Spalla, M.I. (Eds.). 3rd Workshop on Alpine Geological Studies, Padova, pp. 155–176.

Dal Piaz, G.V., Gosso, G., Pennacchioni, G., Spalla, M.I., 1993. Geology of eclogites and related rocks in the Alps. In: Morten, L. (Ed.). Italian Eclogites and Related Rocks, pp. 17–58 Rome, scritti e documenti 13.

Droop, G.T.R., Lombardo, B., Pognante, U., 1990. Formation and distribution of eclogite facies rocks in the Alps. In: Carswell, D.A. (Ed.). Formation and distribution of eclogite facies rocks in the Alps.. Blackie, London, pp. 225–259.

Drury, M.R., Urai, J.L., 1990. Deformation-related recrystallization processes. Tectonophysics 172, 235–256.

Duchéne, S., Blichert-Toft, J., Luais, B., Téluk, P., Lardeaux, J.-M., Albaréde, F., 1997. The Lu–Hf dating of garnets and the ages of the Alpine high-pressure metamorphism. Nature 387, 586–589.

Eckert, J.O., Newton, R.C., Kleppa, O.J., 1991. The ΔH of reaction and recalibration of garnet–pyroxene–plagioclase–quartz geobarometers in the CMAS system by solution calorimetry. American Mineralogist 76, 148–160.

Ellis, D.J., Green, E.H., 1979. An experimental study of the effect of Ca upon garnet clinopyroxene Fe–Mg exchange equilibria. Contributions Mineralogy and Petrology 71, 13–22.

Egydio-Silva, M., Mainprice, D., 1999. Determination of stress directions from plagioclase fabrics in high grade deformed rocks (Além Paraíba shear zone, Ribeira fold belt, southeastern Brazil). Journal of Structural Geology 21, 1751–1771.

Faryad, S.W., 1997. Petrologic and geochronologic constraints on the tectonometamorphic evolution of the Meliata unit blueschists, Western Carpathians (Slovakia). In: Grecula, P., Hovorka, D., Putiš, M. (Eds.). Geological evolution of the Western Carpathians, pp. 145–154 Mineralia Slovaca — Monograph, Bratislava.

Ferrill, D.A., 1991. Calcite twin widths and intensities as metamorphic indicators in natural low-temperature deformation of limestone. Journal of Structural Geology 13 (6), 667–675.

Froitzheim, N., Schmid, S.M., Frey, M., 1996. Mesozoic paleogeography and the timing of eclogite-facies metamorphism in the Alps: a working hypothesis. Tectonophysics 285, 183–209.

Gebauer, D., Tilton, G.R., Schertl, H.P., Schreyer, W., 1993. Eocene/Oligocene ultrahigh-presssure (UHP) — metamorphism in the Dora Maira Massif (Western Alps) and its geodynamic implications. Terra Nova Abstract Supplement 4, 10.

Gleason, G.C., Tullis, J., 1993. The role of dynamic recrystallization in the development of lattice preferred orientations in experimentally deformed quartz aggregates. Journal of Structural Geology 15, 1145–1168.

Godard, G., van Roemund, H.L.M., 1995. Deformation-induced clinopyroxene fabrics from eclogites. Journal of Structural Geology 17, 1425–1443.

Hacker, B.R., Christie, J.M., 1990. Brittle/ductile and plastic/cataclastic transitions in experimentally deformed and metamorphosed amphibolite. Geophysical Monograph 56, 127–147.

Hirth, G., Tullis, J., 1992. Dislocation creep regimes in quartz aggregates. Journal of Structural Geology 14, 145–159.

Hoke, L., 1990. The Altkristallin of the Kreuzeck Mountains, SE Tauern Window, Eastern Alps — basement crust in a convergent plate boundary zone. Jahrbuch Geologische Bundesanstalt 133, 5–87.

Holland, T.J.B., 1980. The reaction albite = jadeite + quartz determined experimentally in the range 600–1200 grad. C. American Mineralogist 65, 129–134.

Jensen, L.N., Starkey, J., 1985. Plagioclase microfabrics in a ductile shear zone from the Jotun Nappe, Norway. Journal of Structural Geology 7, 527–539.

Ji, S., Mainprice, D., 1990. Recrystallization and fabric development in plagioclase. Journal of Geology 98, 65–79.

Knipe, R.J., Law, R.D., 1987. The influence of crystallographic orientation and grain boundary migration on microstructural and textural evolution in an *S–C* mylonite. Tectonophysics 135, 155–169.

Korikovsky, S.P., Putiš, M., Kotov, A.B., Salnikova, E.B., Kovach, V.P., 1998. High-pressure metamorphism of the phengite gneisses of the Lower Austroalpine nappe complex in the Eastern Alps: mineral equilibria, *P–T* parameters, age. Petrology 6, 603–619.

Koziol, A.M., 1989. Recalibration of the garnet–plagioclase–Al2SiO5–quartz (GASP) geobarometer and application to natural parageneses. EOS Transections of American Geophysical Union 70, 493.

Kozur, H., 1991. The evolution of the Meliata–Hallstatt ocean and its significance for the early evolution of the Eastern Alps and Western Carpathians. Palaeogeography, Palaeoclimatology, Palaeoecology 83, 109–135.

Kozur, H., Mock, R., 1973. Zum Alter und zur tektonischen Stellung der Meliata–Serie des Slowakischen Karstes. Geologický Zborník — Geologica Carpathica 24, 365–374.

Kretz, R., 1983. Symbols for rock-forming minerals. American Mineralogist 68, 277–279.

Krogh, E.J., 1988. The garnet–clinopyroxene Fe–Mg geothermometer: a reinterpretation of existing experimental data. Contributions to Mineralogy and Petrology 99, 44–48.

Kümel, F., 1935. Die Sieggrabener Deckscholle im Rosaliengebirge (Nieder Österreich–Burgenland). Tschermaks Mineralogische und Petrographische Mitteilungen 47, 141–184.

Kurz, W., Neubauer, F., 1998. Eclogite meso- and microfabrics: implications for the burial and exhumation history of eclogites in the Tauern Window (Eastern Alps) from *P–T–d* paths. Tectonophysics 285, 183–209.

Leake, B.E. and 21 members of the Subcommittee on Amphiboles, 1997. Nomenclature of amphiboles. Report of the Subcommittee on Amphiboles of the International Mineralogical Association Commission on New Minerals and Mineral Names. European Journal of Mineralogy, 623–651.

Lister, G.S., Hobbs, B.E., 1980. The simulation of fabric development during plastic deformation and its application to quartzite: the influence of deformation history. Journal of Structural Geology 2, 355–370.

Massonne, H.-J., Schreyer, W., 1987. Phengite geobarometry based on the limiting assemblage with K-feldspar, phlogopite and quartz. Contributions to Mineralogy and Petrology 96, 212–224.

Neubauer, F., 1994. Kontinentkollision in den Ostalpen. Geowissenschaften 12, 136–140.

Neubauer, F., Müller, W., Peindl, P., Mozschewitz, E., Wallbrecher, E., Thöni, M., 1992. Evolution of lower Austroalpine units along the eastern margins of the Alps: a review. In: Neubauer, F. (Ed.). ALCAPA Field Guide. University of Graz, pp. 97–114.

Nicolas, A., Poirier, J.P., 1976. Crystalline Plasticity and Solid State Flow in Metamorphic Rocks. J. Wiley & Sons, London, New York, pp. 216–222.

Oberhänsli, R., 1994. Subducted and obducted ophiolites of the Central Alps: paleotectonic implications deduced by their distribution and metamorphic overprint. Lithos 33, 109–118.

Olsen, T.S., Kohlstedt, D.L., 1985. Natural deformation and recrystallization of some intermediate plagioclase feldspars. Tectonophysics 11, 107–131.

Oxburg, E.R., Lambert, R.St.J., Baardsgaard, H., Simons, J.G., 1966. Potassium Argon age studies across the southeast margin of the Tauern Window, the Eastern Alps. Verhandlungen Geologische Bundesanstalt, 17–33.

Perchuk, L.L., 1989. Intercorrelation of Fe–Mg geothermometers using the Nernst law. Geokhimia 5, 611–622 (in Russian).

Perkins, D., Newton, R.C., 1981. Charnockite geobarometers based on coexisting garnet–pyroxene–plagioclase–quartz. Nature 292, 144–146.

Philippot, P., van Roemund, H.L.M., 1992. Deformation processes in eclogitic rocks: evidence for the rheological delamination of the oceanic crust in deeper levels of subduction zones. Journal of Structural Geology 14, 1059–1077.

Platt, J.P., 1993. Exhumation of high-pressure rocks: a review of concepts and processes. Terra Nova 5, 119–133.

Poirier, J.P., Guillopé, M., 1978. Deformation induced recrystallization of minerals. Bulletin Societe fr. Minér. Cristallogr. 102, 67–74.

Powell, R., 1985. Regression diagnostics and robust regression in geothermometer/geobarometer calibration: the garnet–clinopyroxene geothermometer revised. Journal of Metamorphic Geology 3, 327–342.

Plašienka, D., Grecula, P., Putiš, M., Hovorka, D., Kováč, M., 1997. Evolution and structure of the Western Carpathians: an overview. In: Grecula, P., Hovorka, D., Putiš, M. (Eds.). Geological Evolution of the Western Carpathians, pp. 1–24i Mineralia Slovaca — Monograph, Bratislava.

Putiš, M., 1991. Tectonic styles and Late Variscan — Alpine evolution of the Tatric–Veporic crystalline basement in the Western Carpathians. Zentralblatt für Geologie und Paläontologie 1 (1), 181–204.

Putiš, M., 1992. Bericht 1991 Über geologische Aufnahmen im kristallinen Grundgebirge auf Blatt 107 Mattersburg. Jahrbuch Geologische Bundesanstalt 135, 725–726.

Putiš, M., Filová, I., Korikovsky, S.P., Kotov, A.B., Madarás, J., 1997a. Layered metaigneous complex of the Veporic basement with features of the Variscan and Alpine thrust tectonics (the Western Carpathians). In: Grecula, P., Hovorka, D., Putiš, M. (Eds.). Geological Evolution of the Western Carpathians, pp. 175–196 Mineralia Slovaca — Monograph, Bratislava.

Putiš, M., Bezák, V., Kohút, M., Kováčik, M., Marko, F., Plašienka, D., 1997b. Bericht 1996 and 1997 über geologische Aufnahmen im Kristallin auf Blatt 181 Obervellach. Jahrbuch Geologische Bundesanstalt 140, 345–348.

Putiš, M., Fritz, H., Unzog, W., Wallbrecher, E., Korikovsky, S.P., Pushkarev, Y.D., Kotov, A.B., 1998. Exhumation modes of austroalpine eclogite-bearing complexes in the vicinity of penninic windows, Eastern Alps. Abstracts of the XVI Congress of the Carpathian–Balkan Geological Association, Vienna, Austria, p. 501.

Putiš, M., Korikovsky, S.P., Pushkarev, Yu.A., 2000. Petrotectonics of an Austroalpine eclogite-bearing complex (Sieggraben, Eastern Alps) and U–Pb dating of exhumation. Jahrbuch Geologische Bundesanstalt 142, 73–93.

Ring, U., 1992. The Alpine geodynamic evolution of Penninic nappes in the Eastern Central Alps: geothermo–barometric and kinematic data. Journal of Metamorphic Geology 10, 33–53.

Rubie, D.C., 1990. Role of kinetics in the formation and preservation of eclogites. In: Carswell, D.A. (Ed.). Eclogite Facies Rocks. Blackie, Glasgow, pp. 11–140.

Schmid, S.M., Casey, M., 1986. Complete fabric analysis of some commonly observed quartz *c*-axis patterns. In: Hobbs, B.E., Heard, H.C. (Eds.). Mineral and Rock Deformation: Laboratory Studies, pp. 263–286 Geophysical Monograph Series 36.

Schmid, S.M., Paterson, M.S., Boland, J.N., 1980. High temperature flow and dynamic recrystallization in Carrara marble. Tectonophysics 65, 245–280.

Spalla, M.I., Lardeax, J.M., Dal Piaz, G.V., Gosso, G., Messiga, B., 1996. Tectonic significance of Alpine eclogites. Journal of Geodynamics 21, 257–285.

Thöni, M., Jagoutz, E., 1993. Isotopic constraints for eo-Alpine high-P metamorphism in the Austroalpine nappes of the Eastern Alps: bearing on Alpine orogenesis. Schweizerische Mineralogische Petrographische Mitteilungen 73, 177–189.

Tollmann, A., 1977. Geologie von Österreich. Band I: Die Zentralalpen. Deuticke, Vienna.

Trimby, P.W., Prior, D.J., Wheeler, J., 1998. Grain boundary hierarchy development in a quartz mylonite. Journal of Structural Geology 20, 917–935.

Tullis, J., Yund, R.A., 1985. Dynamic recrystallization of feldspar: a mechanism for ductile shear zone formation. Geology 13, 238–241.

Urai, J.L., Means, W.D., Lister, G.S., 1986. Dynamic recrystallization of

minerals. In: Hobbs, B.E., Heard, H.C. (Eds.). Mineral and Rock Deformation: Laboratory Studies — The Paterson Volume, pp. 161–199 American Geophysical Union Geophysical Monograph 36.

Wilson, C.J.L., 1975. Preferred orientation in quartz ribbon mylonites. Geological Society of America Bulletin 86, 968–974.

Zimmermann, R., Hammerschmidt, K., Franz, G., 1994. Eocene high pressure metamorphism in the Penninic units of the Tauern Window (Eastern Alps): evidence from ^{40}Ar–^{39}Ar dating and petrological investigations. Contributions Mineralogy and Petrology 117, 175–186.